The saturation scale and its x-dependence from Lambda polarization studies

Boer, D.; Utermann, A.; Wessels, E.

published in
Physics Letters B
2009

DOI (link to publisher)
10.1016/j.physletb.2008.12.004

document version
Publisher's PDF, also known as Version of record

Physics Letters B 671 (2009) 91–98

Contents lists available at ScienceDirect

Physics Letters B

www.elsevier.com/locate/physletb

The saturation scale and its x-dependence from Λ polarization studies

Daniël Boer, Andre Utermann *,[1], Erik Wessels

Department of Physics and Astronomy, Vrije Universiteit Amsterdam, De Boelelaan 1081, 1081 HV Amsterdam, The Netherlands

ARTICLE INFO

Article history:
Received 12 November 2008
Accepted 4 December 2008
Available online 7 December 2008
Editor: A. Ringwald

PACS:
12.38.-t
13.85.Ni
13.87.Fh
13.88.+e

ABSTRACT

The transverse polarization of forward Λ hyperons produced in high-energy p–A collisions is expected to display an extremum at a transverse momentum around the saturation scale. This was first observed within the context of the McLerran–Venugopalan model which has an x-independent saturation scale. The extremum arises due to the k_t-odd nature of the polarization-dependent fragmentation function, which probes approximately the derivative of the dipole scattering amplitude. The amplitude changes most strongly around the saturation scale, resulting in a peak in the polarization. We find that the observation also extends to the more realistic case in which the saturation scale Q_s is x-dependent. Since a range of x and therefore Q_s values is probed at a given transverse momentum and rapidity, this result is *a priori* not expected. Moreover, the measurement of Λ polarization over a range of x_F values actually provides a direct probe of the x-dependence of the saturation scale. This novel feature is demonstrated for typical LHC kinematics and for several phenomenological models of the dipole scattering amplitude. We show that although the measurement will be challenging, it may be feasible at LHC. The situation at RHIC is not favorable, because the peak will likely be at too low transverse momentum of the Λ to be a trustworthy measure of the saturation scale.

1. Introduction

It is well known that Λ hyperons produced in collisions of unpolarized hadrons are to a large degree polarized perpendicularly to the production plane. Even though the origin of this phenomenon has not been clarified fully yet, for sufficiently large transverse momentum p_t of the Λ, one expects that a parton description must be applicable. In Ref. [1] it was shown that the available Λ polarization data for $p_t > 1$ GeV can be described within a factorized approach by employing a polarization and transverse momentum-dependent fragmentation function. This function, denoted by $\Delta^N D$, describes the fragmentation of an unpolarized quark into a transversely polarized Λ and is an odd function of the transverse momentum k_t of the quark w.r.t. the Λ momentum [2]. This k_t-odd nature implies that it is essentially accompanied by the first derivative of the partonic cross section w.r.t. k_t, unlike the unpolarized Λ fragmentation function D, which is k_t-even. This turns the observed Λ polarization into a useful tool, which in this Letter will be applied to the study of the x-dependence of the saturation scale.

Once the polarization-dependent fragmentation function is known from data in the large x or DGLAP region, polarization measurements in other kinematic regions could point to changes in the underlying physics. In Ref. [3] this was discussed specifically for the saturation region, the region of small momentum fraction x where the gluon density is very high and is expected to saturate according to the nonlinear evolution equations of relevance in that region. The saturation region is characterized by the so-called saturation scale Q_s, i.e. the momentum scale at which saturation effects become sizable. It was noted within the context of the McLerran–Venugopalan model [4], which has an x-independent saturation scale Q_s, that the negative valued Λ polarization displays a minimum at a transverse momentum approximately equal to Q_s. Here, we want to investigate the more realistic case in which the saturation scale is x-dependent [5–7]. It may be expected that, since now a range of Q_s-values is probed, the minimum of the polarization is smeared out, and possibly not recognizable anymore. However, in this Letter we will demonstrate that this is not the case. In fact, the pronounced minimum of the polarization can even be used to probe the x-dependence of the saturation scale. This makes the observable of potential interest for collider experiments at RHIC, LHC and a future electron–ion collider, the EIC.

Having discussed this promising use of Λ polarization, let us now address the possibilities of measuring it in the small-x region. In high energy scattering the polarization of a spin-1/2 final state hadron can usually only be measured through self-analyzing par-

* Corresponding author.
E-mail addresses: d.boer@few.vu.nl (D. Boer), andre.utermann@physik.uni-regensburg.de (A. Utermann), e.wessels@few.vu.nl (E. Wessels).
[1] Present address: Institut für Theoretische Physik, Universität Regensburg, D-93040 Regensburg, Germany.

0370-2693/$ – see front matter
doi:10.1016/j.physletb.2008.12.004

ity violating decays. Exploiting this property it was demonstrated already more than 30 years ago [8,9] that Λ hyperons emerging from unpolarized p–A collisions are polarized perpendicularly to the production plane (cf. Ref. [10] for an extensive review of data). In the fixed target experiments performed at typical center of mass energies $\sqrt{s} \sim 20$ GeV, the transverse momentum dependence of the degree of polarization shows the characteristic feature that after a linear rise up to $p_t \sim 1$ GeV, it stays remarkably constant up to the highest measured values $p_t \sim 4$ GeV. This behavior was found to be independent of the specific values of $\sqrt{s}$ and atomic number A. For larger p_t values one expects the asymmetry to fall off as $1/p_t$, but this has not been observed yet. None of the measurements performed thus far are in a kinematic region where the target could be considered dense, i.e. in the saturation region. In Ref. [3] it was pointed out that the characteristic flat behavior observed for p_t values of a few GeV, would in that case no longer be present, but rather an extremum should be visible, located at $p_t \sim Q_s$. In other words, the observed plateau should turn into a peak as saturation effects set in and Q_s becomes a relevant scale. Since Q_s grows with $1/x$ and A, one expects this to happen when $\sqrt{s}$ and/or A are increased significantly. In addition, it also helps to consider large rapidities, i.e. forward Λ production, in order to decrease the x values probed. At RHIC forward Λ's with rapidities of around 4 would begin to probe the small-x region according to a dipole scattering description [11]. The possibilities to probe small x-values are of course greater at LHC, where due to the much higher $\sqrt{s}$ much less forward Λ's are required. For completeness, we recall that at RHIC d–Au collisions have been studied at energies of ~ 200 GeV/A in the nucleon–nucleon center of mass frame. At LHC p–Pb collisions will be performed at $\sqrt{s_{NN}} = 8.8$ TeV, but these do not take place in the nucleon–nucleon center of mass frame which leads to a rapidity shift from lab frame to center of rapidity frame of about half a unit. In principle also the p–p collisions at LHC are of interest here, due to the very large energy: $\sqrt{s} = 14$ TeV.

Experimentally the measurement of forward Λ's and their polarization may be hampered by the often restricted particle identification capabilities in the forward region. Two-thirds of the time Λ's decay into protons and negatively charged pions: $\Lambda \to p\pi^-$. The angular distribution of the decay in the Λ rest frame is used to determine the polarization of the Λ. Unfortunately, protons are usually hard to identify in the forward region. In that case the only alternative may be to use that the Λ's decay one third of the time into neutrons and neutral pions (and subsequently, two photons): $\Lambda \to n\pi^0 \to n\gamma\gamma$. Neutrons, π^0's and photons have been identified in the forward region at RHIC, hence this alternative may be feasible [12] and may in fact be the only way of measuring Λ polarization in the forward region at RHIC, LHC or EIC. We will proceed with our investigation under the assumption that forward Λ polarization measurements will be possible in the future.

The outline of this Letter is as follows. In Section 2 we discuss the Λ polarization asymmetry in terms of the relevant polarization-dependent fragmentation function and the dipole scattering amplitude. This discussion repeats the essentials from Ref. [3] in order to set the notation and to explain why an extremum is expected at $p_t \propto Q_s$, but also it includes the details of various phenomenological models for the dipole scattering amplitude that were considered in the literature. As mentioned, in Ref. [3] only the McLerran–Venugopalan model was considered, but here we will focus on more recent models that employ an x-dependent saturation scale. In Section 3 we discuss model results for the Λ polarization observable for LHC kinematics mainly and point out the generic qualitative features. Achieving realistic quantitative predictions for the degree of Λ polarization will not be our aim, due to the large uncertainty in the polarization-dependent fragmentation function. Nevertheless, an estimate can be given of the range of x_F values required to observe the x-dependence of the saturation scale, as the p_t-dependence of the Λ polarization is found to be less model-dependent than its absolute value. Prospects for RHIC are also briefly discussed, but no results will be shown. The reason for this is that at RHIC the peak is likely situated at a p_t below 1 GeV, where the considered framework would not be appropriate. We end with conclusions.

2. Transverse Λ polarization description at small x

According to Ref. [3], the transverse polarization of forward Λ's produced in unpolarized p–A collisions is approximately given by

$$\begin{aligned}
&\mathcal{P}_\Lambda(p_t, x_F) \\
&= \left\{ \int_{x_F}^1 \mathrm{d}x\, x \sum_q f_{q/p}\big(x,\mu_f^2\big)\Delta^N D_{\Lambda^\uparrow/q}\left(\frac{x_F}{x},\mu_f^2\right) \right. \\
&\quad \left. \times \left[N_F\left(\frac{x}{x_F}\big(p_t - k_t^0\big), x_2\right) - N_F\left(\frac{x}{x_F}\big(p_t + k_t^0\big), x_2\right)\right]\right\} \\
&\quad \times \left\{ \int_{x_F}^1 \mathrm{d}x \left[\sum_q f_{q/p}\big(x,\mu_f^2\big) D_{\Lambda/q}\left(\frac{x_F}{x},\mu_f^2\right) N_F\left(\frac{x}{x_F}p_t, x_2\right)\right.\right. \\
&\quad \left.\left. + f_{g/p}\big(x,\mu_f^2\big) D_{\Lambda/g}\left(\frac{x_F}{x},\mu_f^2\right) N_A\left(\frac{x}{x_F}p_t, x_2\right)\right]\right\}^{-1}, \qquad (1)
\end{aligned}$$

where y_h and p_t are the rapidity and the transverse momentum of the produced Λ, $x_F = p_t/\sqrt{s}\exp[y_h]$, and x and $x_2 = q_t^2/(xs)$ are respectively the momentum fractions of the parton in the proton and the heavy ion (referred to as the "target"). Note that three different values of x_2 enter in this polarization expression, in conjunction with the three different transverse momenta $q_t = x/x_F(p_t \pm k_t^0)$ and $q_t = x/x_F p_t$ of the scattered parton. The expression (1) is based on the asymmetry expression of Ref. [1] combined with the dipole picture description of the cross section of Ref. [11]. In the dipole formalism, N_F describes the scattering of a quark off a nucleus, while N_A describes gluon–nucleus scattering. For details of the derivation and justification of the approximations we refer to Ref. [3], where the dipole scattering amplitude N_F is denoted by C.

The polarization-dependent fragmentation function $\Delta^N D_{\Lambda^\uparrow/q}$ is parameterized in terms of the unpolarized one $D_{\Lambda/q}$ of Ref. [13],

$$\Delta^N D_{\Lambda^\uparrow/q}\big(z,\mu^2\big) \equiv f_q^\Delta(z) D_{\Lambda/q}\big(z,\mu^2\big), \qquad (2)$$

where

$$\begin{aligned}
&f_q^\Delta = \frac{1}{2} N_q z^{c_q}(1-z)^{d_q}, \qquad N_u = N_d = -28.13, \\
&N_s = 57.53, \qquad c_q = 11.64, \qquad d_q = 1.23, \qquad (3)
\end{aligned}$$

and the average transverse momentum is given by

$$k_t^0(z) = 0.66 z^{0.37}(1-z)^{0.5}\ \text{GeV}. \qquad (4)$$

We emphasize that there is a large uncertainty in this parameterization extracted from fixed target data [1], so that the numerical results presented below should only be viewed as qualitative, not as quantitative predictions. Future collider data from LHC could be used to obtain a more trustworthy parameterization, for instance through the Λ + jet observable recently pointed out in Ref. [14], which deals with Λ's at midrapidity where particle identification does not pose a problem.

Using the McLerran–Venugopalan (MV) model for the dipole scattering amplitude it was shown in [3] that the p_t distribution of the transverse polarization displays a peak that is directly related

to the saturation scale Q_s. However, the MV model does not incorporate evolution in x; Q_s is constant. Here we want to investigate whether $\mathcal{P}_\Lambda$ as a function of p_t still possesses an observable peak when described using a more realistic dipole scattering amplitude including x-evolution. A phenomenologically successful model with an x-dependent Q_s is the Golec-Biernat and Wüsthoff (GBW) model [15], which was able to describe small-x DIS data.[2] Here we will focus on two different modifications of the GBW model that were introduced to describe RHIC d–Au data: the DHJ model [17,18] and the geometric scaling (GS) model of Ref. [19]. Both are of the form

$$N_F(q_t, x_2) \equiv \int \mathrm{d}^2 r_t\, e^{i\vec{q}_t\cdot\vec{r}_t}\left[1-\exp\left(-\frac{1}{4}\left(\frac{4}{9}r_t^2 Q_s^2(x_2)\right)^{\gamma(q_t,x_2)}\right)\right], \tag{5}$$

where N_A is obtained from N_F by replacing $\frac{4}{9}r_t^2 Q_s^2(x_2)$ by $r_t^2 Q_s^2(x_2)$, and the saturation scale is given by [15]

$$Q_s(x_2) = (1\ \mathrm{GeV})\left(\frac{x_0}{x_2}\right)^{\lambda/2}, \tag{6}$$

where the parameters $x_0 \simeq 3\times 10^{-4}$ and $\lambda \simeq 0.3$ were fitted to the small-x DIS data. In the GBW model the so-called anomalous dimension γ is simply equal to 1. The DHJ model incorporates expectations on the behavior of γ from BFKL/BK evolution [17,18], namely a logarithmic dependence on $q_t^2/Q_s^2(x)$, and violations of geometric scaling that are proportional to $1/y$ (at large y)

$$\gamma_{\mathrm{DHJ}}(q_t, x_2) = \gamma_s + (1-\gamma_s)\frac{|\log(q_t^2/Q_s^2(x_2))|}{\lambda y + d\sqrt{y} + |\log(q_t^2/Q_s^2(x_2))|}, \tag{7}$$

where $\gamma_s = 0.6275$, $y = \log 1/x_2$ is minus the rapidity of the target parton. The saturation scale $Q_s(x)$ and the parameter λ are taken from the GBW model, as given in Eq. (6), and $d = 1.2$ was fitted to data. Here Q_s includes the additional factor $A^{1/3}$, where for large atomic numbers A usually a lower, effective number A_{eff} is used to account for impact parameter-dependence.

The parameterization of γ_{DHJ}, which is based on the one given in Ref. [20], is well motivated by expectations from small-x evolution that are valid only for $q_t \geqslant Q_s$ [6,21]. In contrast, the continuation to the saturation region $q_t \leqslant Q_s$ is rather undetermined. In the case of hadron production at RHIC [17,18] this is not crucial since this region is hardly probed. But the polarization observable discussed here is sensitive to γ around Q_s, not only to $q_t \geqslant Q_s$. Hence, the continuation of γ to the saturation region affects the polarization around the peak.

The DHJ model was found to describe well forward hadron production in d–Au collisions at RHIC, but it fails at central rapidity [19]. In particular, the logarithmic rise of γ proved to be too slow to describe the larger x central rapidity data. Also the scaling violations of the DHJ model could not be resolved in the data. In order to investigate to what extent the RHIC data establish the small-x properties incorporated in the DHJ model, a new model was put forward that is not only exactly geometrically scaling, but in addition features a stronger rise of γ [19]

$$\gamma_{\mathrm{GS}}(w) = \gamma_s + (1-\gamma_s)\frac{(w^a-1)}{(w^a-1)+b}. \tag{8}$$

Here, $a = 2.82$ and $b = 168$ were fitted to the data. This GS model turned out to be able to describe the d–Au data well at all rapidities. It must be emphasized though that when restricted to the forward data, or equivalently the smaller x data, both models describe the data equally well. From the comparison of the model predictions to future LHC p–Pb and p–p data one should be able to learn which rise is more appropriate at small x. Given this uncertainty, here we will use both models to study the transverse Λ polarization.

To shed light on the peak in the p_t distribution, we will separate $\mathcal{P}_\Lambda$ into a p_t-dependent and an x_F-dependent part in the following way. To good approximation the integrals in (1) are dominated by a value of $x_F/x \equiv z$ that is independent of p_t and only moderately dependent on x_F. Due to the large power c_q, which suppresses small ratios z in the numerator, the z effectively probed in the numerator and the denominator are different. We will denote the value that dominates the numerator with z and the smaller one that dominates the denominator with z'. Of course in the kinematic limit $x_F \to 1$, both z and z' must become equal to 1. In the following analysis we will stay away from this limit and assume that x_F stays smaller than roughly 0.5. Ignoring the gluonic contributions, which is a good approximation when x_F is not too small, we can approximate (1) in the following way:

$$\mathcal{P}_\Lambda(p_t, x_F) \approx \frac{\sum_q D_{\Lambda/q}(z)(x_F/z) f_{q/p}(x_F/z, \mu_f^2) f_q^\Delta(z)}{\sum_q D_{\Lambda/q}(z')(x_F/z') f_{q/p}(x_F/z', \mu_f^2)} \times \frac{N_F\left(\frac{1}{z}(p_t-k_t^0), \frac{1}{x_F z}\frac{(p_t-k_t^0)^2}{s}\right) - N_F\left(\frac{1}{z}(p_t+k_t^0), \frac{1}{x_F z}\frac{(p_t+k_t^0)^2}{s}\right)}{N_F\left(\frac{1}{z'}p_t, \frac{1}{x_F z'}\frac{p_t^2}{s}\right)}. \tag{9}$$

Since z and z' are considered constant, Eq. (9) now depends on p_t through the function N_F only. This is true assuming the factorization scale μ_f to be constant. Below we will mostly choose $\mu_f = p_t$ though, but this will turn out not to make much difference. We further note that since k_t^0 is only around 0.3 GeV or smaller for all relevant values of z, we can expand $N_F(\frac{1}{z}(p_t-k_t^0)) - N_F(\frac{1}{z}(p_t+k_t^0))$ in terms of k_t^0/p_t, requiring $p_t \geqslant 1$ GeV throughout this Letter,

$$N_F\left(\frac{1}{z}\left(p_t-k_t^0\right)\right) - N_F\left(\frac{1}{z}\left(p_t+k_t^0\right)\right) \approx -2\frac{k_t^0}{z}\frac{\mathrm{d}N_F}{\mathrm{d}q_t}. \tag{10}$$

Here we have suppressed the explicit dependence on x_2 for convenience and we will do so frequently below. Writing the dipole scattering amplitude in terms of a dimensionless function $\tilde{N}_F$,

$$N_F(q_t, x_2) \equiv \frac{2\pi}{q_t^2}\tilde{N}_F\left(w = q_t/Q_s(x_2), x_2\right), \tag{11}$$

we can express Eq. (10) in the following way:

$$N_F\left(\frac{1}{z}\left(p_t-k_t^0\right)\right) - N_F\left(\frac{1}{z}\left(p_t+k_t^0\right)\right) \approx 2\frac{k_t^0}{p_t}\frac{2\pi}{q_t^2}\left(2\tilde{N}_F(w) - w\tilde{N}_F'(w)\right). \tag{12}$$

Using this result, we can split off the p_t-dependence of the transverse polarization and write

$$\mathcal{P}_\Lambda(p_t, x_F) \approx \frac{\sum_q D_{\Lambda/q}(z)(x_F/z) f_{q/p}(x_F/z, \mu_f^2) f_q^\Delta(z)/z}{\sum_q D_{\Lambda/q}(z')(x_F/z') f_{q/p}(x_F/z', \mu_f^2)} \times \frac{k_t^0}{Q_s}\frac{z^2}{z'^2}F(w, w'), \tag{13}$$

where we have defined the p_t-dependent part of $\mathcal{P}_\Lambda$ as a separate function $F(w, w')$,

$$F(w, w') = \frac{2}{w}\frac{2\tilde{N}_F(w) - w\tilde{N}_F'(w)}{\tilde{N}_F(w')}. \tag{14}$$

[2] Note that the GBW model was found to be inconsistent with newer, more accurate data and requires some modification at larger Q^2, see, for example, Ref. [16].

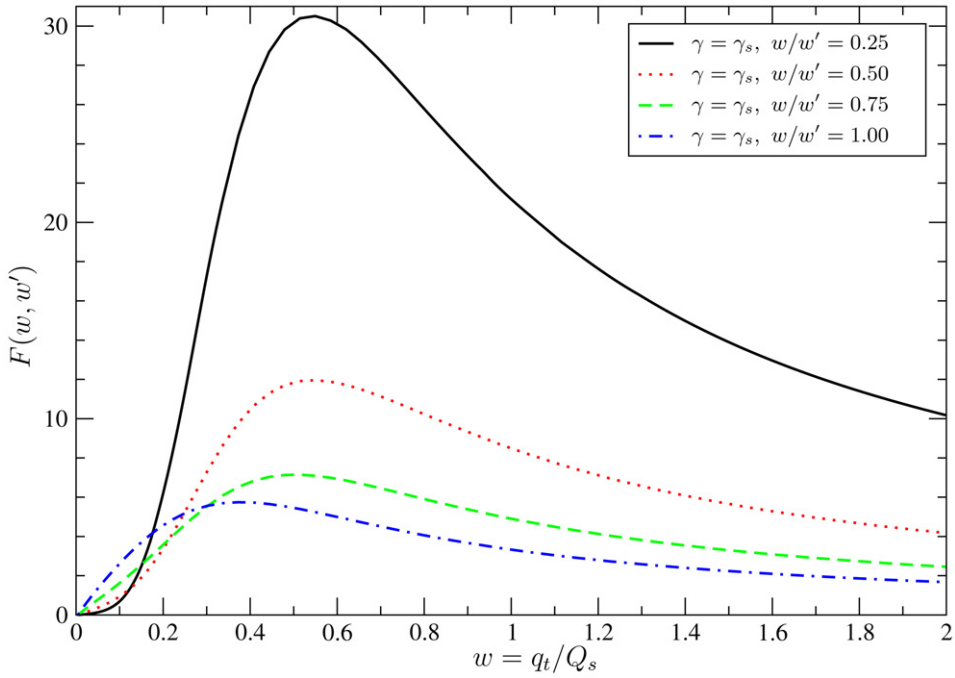

Fig. 1. The function $F(w, w')$ for $\gamma = 0.6275$ and various ratios w/w'.

From the asymptotic behavior of F it can be seen that it must have an extremum. From Eqs. (5) and (11), it follows that $\tilde{N}_F \propto 1/w^{2\gamma}$ for large w, and hence that $F(w, w')$ will approach $2(1+\gamma)/w$. On the other hand, in the deep saturation regime the function (11) is proportional to w^2, so that $F(w, w')$ vanishes as $w \to 0$. Therefore, the function $F(w, w')$, and consequently P_Λ, must have a peak as it connects these two asymptotic behaviors. Without saturation there could also be a peak in P_Λ, but one would in that case not expect the extremum to be rather sharply peaked at a perturbative scale of a few GeV. Such a peak would be a sign of saturation, especially if it increases towards larger transverse momenta with increasing energy. Of course, there could be a plateau-like extremum, as it appears to be the case at low energies. However, the MV model calculation of Ref. [3] clearly shows there to be a pronounced peak, with a position proportional to the (constant) saturation scale Q_s. If this proportionality holds when Q_s evolves with x, the location of the peak in p_t would be a direct probe of the running of Q_s through its dependence on x_F. If however the peak position depends also *explicitly* on x_F, the running of Q_s cannot be reconstructed from the peak position. Because the probed values of $z'/z = w/w'$ depend on x_F, this means that we have to check that they do not influence the position of the peak. Fig. 1 shows $F(w, w')$ for various values of $w/w' = z'/z$ ranging from 0.25 to 1, using a dipole scattering amplitude with a constant $\gamma = 0.6275$. The curves indeed have a clear maximum[3] as a function of w. The position of the peak hardly depends on w'/w if w'/w is not too close to 1, i.e. away from the kinematic limit $x_F \to 1$. Hence, we conclude that the peak of F is located at an approximately constant value of w. As mentioned, this means that the minimum of $\mathcal{P}_\Lambda$ does not explicitly depend on x_F, but only through the saturation scale Q_s.

We find that all this remains true not only for different constant γ's, but also for the DHJ and GS models. The GS model actually leads to the same peak position as constant $\gamma = \gamma_s$, because it differs only little from $\gamma_{\mathrm{GS}}(w = 1) = \gamma_s$ in the saturation region $w \leqslant 1$, where the peak of F is located. The DHJ model gives a slightly different peak, one that depends on the continuation into the saturation region $q_t < Q_s$, as will be discussed further below.

One can estimate the x_F dependence of the peak of the resulting p_t-distribution as follows. Since the peak of F is at a constant value of $w = zp_t/Q_s$, where z is roughly constant as well, the peak in p_t is directly proportional to $Q_s(x)$. Because the dominant value of x that is probed depends on both p_t and x_F, the peak position p_t^{peak} will depend on x_F. As the probed value of $z = x_F/x$ in the integrals in Eq. (1) is to good approximation constant, the target momentum fraction x_2, which sets the saturation scale $Q_s(x_2)$, is given by

$$x_2 = x\exp(-2y_h) = \frac{x}{x_F^2}\frac{p_t^2}{s} \propto \frac{1}{x_F}\frac{p_t^2}{s}. \tag{15}$$

Using this relation, we can estimate the x_F-dependence of the peak position p_t^{peak} of $\mathcal{P}_\Lambda$. Assuming that the saturation scale is given by a power law in $1/x$, Eq. (6), we see that

$$p_t^{\mathrm{peak}} \propto Q_s\big(x_F, p_t^{\mathrm{peak}}\big) \propto Q_0\left(\frac{x_F x_0 s}{(p_t^{\mathrm{peak}})^2}\right)^{\lambda/2} \tag{16}$$

$$\Rightarrow p_t^{\mathrm{peak}}(x_F) \propto Q_0 x_F^{\lambda'/2}\left(\frac{x_0 s}{Q_0^2}\right)^{\lambda'/2}, \quad \lambda' = \frac{\lambda}{1+\lambda}. \tag{17}$$

Hence, we conclude that the running of the peak position with x_F is a clear indication of the running of the saturation scale $Q_s(x_2)$. Moreover, the power λ can be reconstructed from the behavior of the peak position as a function of x_F.

The parameterization of Q_s in Eq. (6) is not just based on the GBW model fit to DIS data. The specific power law dependence on $1/x$ stems from theoretical arguments. Small-x evolution equations, such as the GLR [22], BFKL [23] and BK [24] equations in the fixed coupling constant case, result in such a behavior and determine the power λ (typically they yield $\lambda \approx 0.9$). In the running coupling case the functional form of Q_s is different. But over the limited range of experimentally accessible values of x, Q_s can still

[3] Since the polarized part of the fragmentation function f_q^Δ is negative for the u and d quarks that lead to the dominating contributions, $\mathcal{P}_\Lambda$ will have a negative valued minimum, which for convenience will sometimes also simply be referred to as a peak.

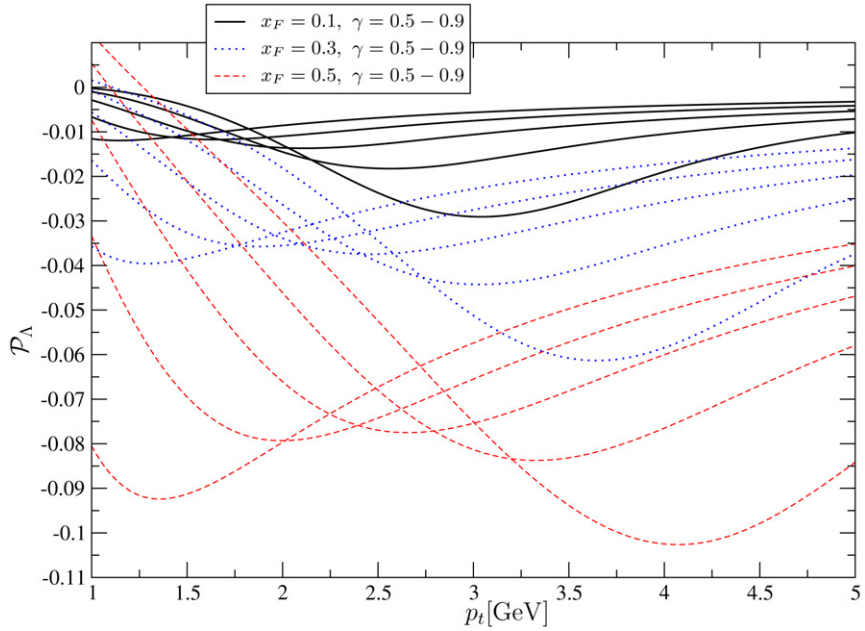

Fig. 2. $\mathcal{P}_\Lambda$ for various constant γ for p–Pb collisions at $\sqrt{s} = 8.8$ TeV. Curves for smaller γ have their minimum at smaller p_t.

be approximated by a power law like behavior. In this way the specific value of $\lambda = 0.3$ that best describes the DIS data, can be effectively accommodated. This implies that λ may be different in p–A collision where a different kinematic range is probed.

In the discussion above we have expanded N_F in terms of k_t^0/p_t requiring $p_t \geqslant 1$ GeV, so that p_t is in the perturbative regime. This should be considered a minimal requirement for the present dipole description to be applicable and also from the perspective of the scale choice $\mu_f = p_t$ it is a sensible lower bound. Therefore, below we will only discuss results for which p_t^{peak} is in the perturbative regime.

3. Transverse Λ polarization results

Here we will present our numerical estimates of the transverse polarization (1). For the fragmentation functions we have chosen the leading order (LO) functions given in [13] and for the parton distributions the CTEQ5 LO ones [25]. In [18] it was shown that certain effects of higher order can be taken into account by the DGLAP evolution of fragmentation functions and parton distributions at the scale set by p_t. Unless stated otherwise, we will therefore set the factorization scale to $\mu_f = p_t$. We will return to the μ_f dependence of the results later on.

We first discuss the p_t distribution of $\mathcal{P}_\Lambda$ for constant values of x_F. Here we will first give the result for p–Pb collisions at LHC at $\sqrt{s} = 8.8$ TeV explicitly and later point out how they compare to p–p collisions at LHC and d–Au collisions at RHIC. For the saturation scale we will use the GBW parameterization (6) with $Q_0^2 = 2.7$ GeV^2 instead of 1 GeV^2 by taking $A_{\text{eff}} = 20$. Fig. 2 shows the resulting $\mathcal{P}_\Lambda$. It has been calculated for dipole scattering amplitudes with various constant values of γ from 0.5 to 0.9. The increasing magnitude of the polarization with increasing x_F is due to the polarized part of the fragmentation f_q^Δ (for larger x_F larger values of z are probed). The anticipated rise of the peak position with x_F can be clearly observed. Furthermore, the peak position rises approximately linearly with γ for all considered values of x_F.

Fig. 3 shows the polarization for various x_F as a function of p_t, but now for three γ's that are all equal at the saturation scale: a constant γ_s, γ_{DHJ} and γ_{GS}. As expected, the difference between the polarization for γ_s and γ_{GS} is very small because in the saturation region γ_{GS} differs only mildly from the value $\gamma_{\text{GS}}(q_t = Q_s) = \gamma_s$. Because of the uncertainty in the continuation of the DHJ parameterization in the saturation region, the estimate of $\mathcal{P}_\Lambda$ around the peak is ambiguous. If we would, for instance, continue γ_{DHJ} by keeping it constant for $q_t < Q_s$, we would obtain roughly the same result as for γ_{GS}. The fact that the DHJ and GS models yield similar results for the observed behavior of the peak indicates our findings are rather robust and to a certain extent model-independent. In contrast, the magnitude of the polarization is subject to considerable uncertainty, mostly due to the parameterization of $\Delta^N D$, but also somewhat due to the choice of the factorization scale.

Thus far we have used a factorization scale $\mu_f = p_t$. However, in Ref. [3] $\mu_f = Q_s$ was considered, which may also be a natural choice. In the present case that would lead to an x-dependent factorization scale. Fig. 4 shows $\mathcal{P}_\Lambda$ with γ_{GS} for three different factorization scales, $\mu_f = p_t$, $\mu_f = Q_s$, and a constant scale $\mu_f = 1$ GeV. As can be seen, for constant x_F the shape of the p_t distributions is rather independent of the factorization scale. The normalization does depend on the choice of μ_f, but still only moderately. Therefore, choosing $\mu_f = p_t$ does not noticeably affect our claim that the x_F-dependence of the peak momentum directly probes the x-dependence of the saturation scale.

Fig. 5 shows the x_F-dependence of the peak position of the p_t distribution for various choices of γ. The lines for constant γ confirm that the peak position scales linearly with γ. Moreover, for not too large x_F, the power law rise of p_t^{peak} with x_F is consistent with the result we obtained in Eq. (17), including the fact that the power is independent of γ. As expected, the results for $\gamma_{\text{GS}}(w)$ (8) and the constant $\gamma = \gamma_s$ are very close to each other. The curve for γ_{DHJ} (7) is similar to that of a constant γ that is slightly larger than γ_s. This is because γ_{DHJ} rises rather quickly in the saturation region as q_t decreases.

As can be seen from Fig. 5 all slopes are also numerically consistent with the power $\lambda'/2$ in Eq. (17) for $\lambda = 0.3$. This implies that an increase in x_F by a factor 5 leads to a shift in the peak position of approximately 20%. This can be seen directly in Fig. 4 too, when comparing the peak position at $x_F = 0.1$ and 0.5. Unfortunately, this is not a large shift, but it does give an estimate for the precision with which the peak position needs to be determined. It should be mentioned that, as discussed before, the value of λ may be different in p–A collisions than the one taken from

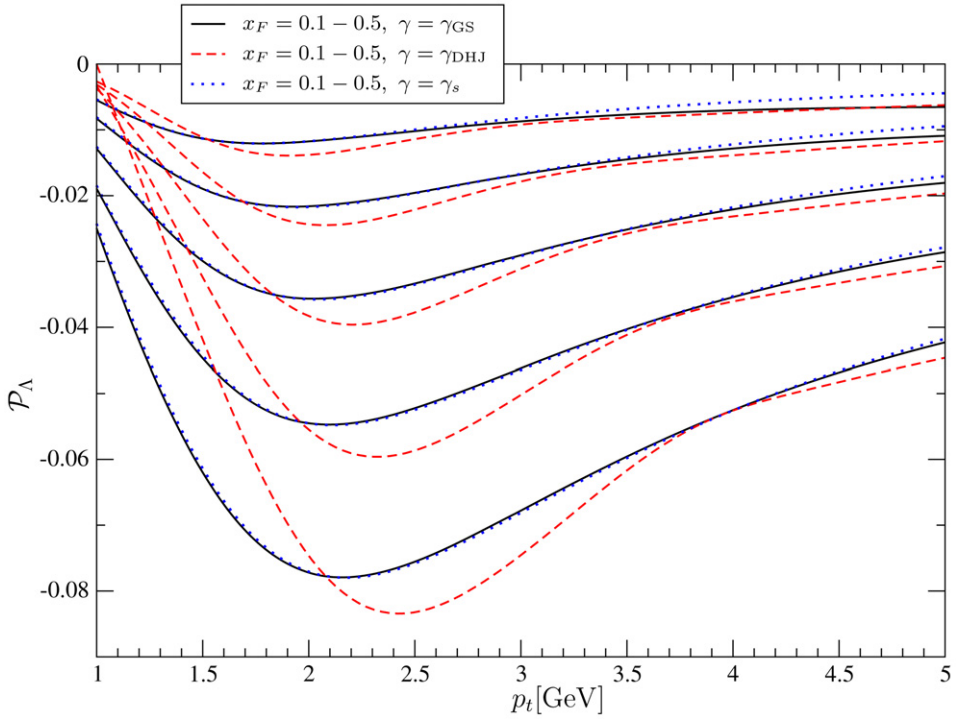

Fig. 3. $\mathcal{P}_\Lambda$ in p–Pb collisions at $\sqrt{s} = 8.8$ TeV, for $\gamma_{\rm DHJ}$, $\gamma_{\rm GS}$ and a constant γ_s. The top lines correspond to $x_F = 0.1$, the lowest to $x_F = 0.5$.

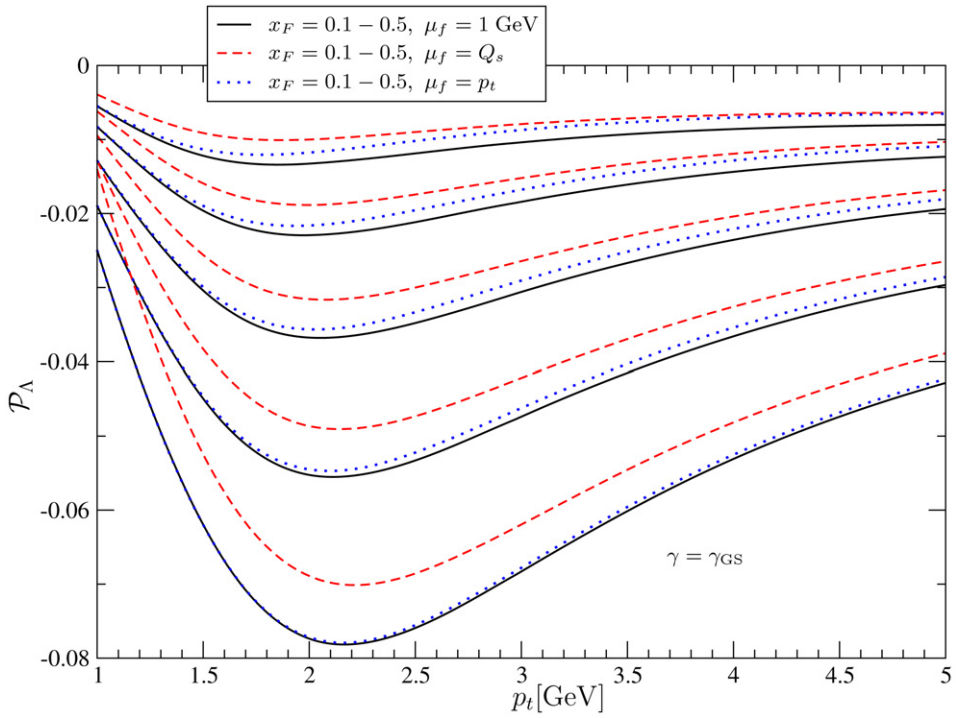

Fig. 4. $\mathcal{P}_\Lambda$ in p–Pb collisions at LHC for the scaling $\gamma_{\rm GS}$ (8) and three different choices of the factorization scale $\mu_f = p_t$, Q_s and 1 GeV. The top lines correspond to $x_F = 0.1$, the lowest to $x_F = 0.5$.

the analysis of the small-x DIS data. A larger value of λ would of course result in a stronger x-dependence of Q_s and therefore in a larger x_F-dependence of the peak position that would be easier to observe. At small x_F, where the position of the peak is less pronounced, it will be harder to determine than at large x_F. The value of p_t/Q_s at which the peak is situated depends – too good approximation linearly – on γ in the saturation region $q_t \leqslant Q_s$. As can be seen in Fig. 3, the peak is located for $\gamma_{\rm GS}$ and $\gamma = \gamma_s$ at almost the same position. We find empirically that in these cases the minimum in the p_t distribution shows up at $w \approx 0.55$, i.e. $p_t \approx 0.55 z Q_s$, where z rises slightly with x_F from 0.7 to 1 in the limit $x_F \to 1$. Depending on the continuation of the DHJ model to the saturation region the peak is situated at a different w. For the continuation (7) the peak shows up at $p_t \approx 0.60 z Q_s$, since it rises again towards smaller q_t in the saturation region.

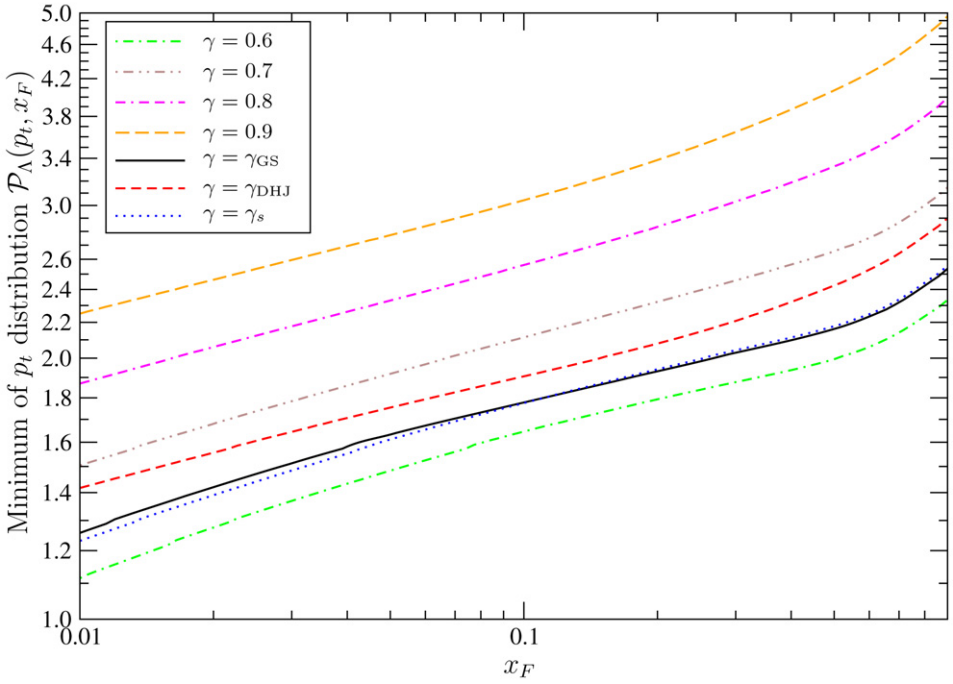

Fig. 5. The peak position of the p_t distribution $\mathcal{P}_\Lambda(p_t, x_F)$ as a function of x_F in double logarithmic representation for various choices of γ.

Similar results for $\mathcal{P}_\Lambda$ are obtained for p–p collisions at LHC and d–Au collisions at RHIC. Again an extremum is observed at around one half times the saturation scale that shows the same x_F-dependence as for p–Pb scattering at LHC. However, due to the different kinematics and targets, Q_s and hence the position of the peak $p_t^{\rm peak}$ is in both cases lower. Following the same line of arguments leading to the x_F-dependence of $p_t^{\rm peak}$ (17), one can estimate its $\sqrt{s}$- and Q_0-dependence,

$$p_t^{\rm peak}(x_F, \sqrt{s'}, Q_0') = p_t^{\rm peak}(x_F, \sqrt{s}, Q_0)\left(\frac{Q_0'(\sqrt{s'})^\lambda}{Q_0(\sqrt{s})^\lambda}\right)^{1/(1+\lambda)}. \quad (18)$$

For p–p at LHC Q_0 is 1 GeV and $\sqrt{s} = 14$ TeV. Hence, the peak position is expected to be reduced by a factor of 1.3 with respect to p–Pb collisions at $\sqrt{s} = 8.8$ TeV. An explicit calculation confirms that this estimate works very well, i.e. the x_F-dependent extremum is expected to show up approximately between 1.5 and 2.0 GeV for $x_F \sim 0.1$–0.5. For d–Au collisions at RHIC the probed values of x_2 are less small due to the smaller energy. Hence, the probed values of Q_s and hence $p^{\rm peak}$ are reduced even more, namely by a factor of 2.4 compared with p–Pb collisions at LHC, which may situate it below the perturbative regime $p_t \gtrsim 1$ GeV, even for constant values of $x_F = 0.1$–0.5. However, given the uncertainties in e.g. the values of Q_0 and λ, a peak in the perturbative region is not ruled out, especially for larger x_F. From this perspective it may still be worthwhile to investigate this observable at RHIC.

Up to now we focused on the calculation of $\mathcal{P}_\Lambda$ at constant x_F, where the dependence on $\sqrt{s}$ is not that large. However, from an experimental point of view it might be more convenient to measure $\mathcal{P}_\Lambda$ for constant rapidities y_h. As demonstrated before, there is a clear peak in the p_t distribution at fixed x_F, which is at different locations for different x_F. Therefore, since at fixed y_h a range of values of x_F contributes, the peak will be smeared out to some extent (this can also be observed for the DHJ model predictions of single spin asymmetries in forward pion production in the collisions of transversely polarized protons with unpolarized protons [26]). Hence, it is not clear *a priori* whether the peak remains observable and whether the peak position is still a clear probe of the saturation scale.

For LHC kinematics, we know from the previous analysis that a peak at transverse momenta larger than 1 GeV requires $x_F = p_t/\sqrt{s}\exp[y_h] \gtrsim 0.01$. At LHC such a peak is thus only expected in the forward region $y_h \gtrsim 4$. Fig. 6 shows $\mathcal{P}_\Lambda$ for p–Pb scattering at LHC at $\sqrt{s_{NN}} = 8.8$ TeV, for values of $y_h = 4, 5, 6$. Indeed, the extremum is in these cases located at a p_t larger than 1 GeV, but it is much less pronounced than at fixed x_F and for the GS model less recognizable than for the DHJ model. We also note that the magnitude of the asymmetry is considerably reduced compared to the fixed x_F case.

At RHIC the saturation scale becomes roughly of the order $Q_s \gtrsim 1$ GeV for forward Λ's with rapidities of around 4. However, unlike for the MV model, the peak position for the DHJ and GS models is located considerably below Q_s, that is, below $p_t = 1$ GeV. An explicit calculation of P_Λ for RHIC confirms that even for $y_h = 4$ a peak is not expected to be above 1 GeV. In other words, $Q_s(x)$ can presumably not be extracted in a trustworthy manner from a fixed $y_h = 4$ analysis at RHIC, unless Q_0 and/or λ turn out to be larger than expected at present.

4. Conclusions

The transverse polarization of Λ particles displays a peak at the saturation scale when described using the MV model for the dipole scattering amplitude. We find that in the more realistic case where the dipole amplitude depends on x, such a peak in the p_t distribution remains. The position of the peak, $p_t^{\rm peak}$, is still proportional to Q_s, and therefore offers a direct experimental probe of this scale. For fixed values of x_F, the x-dependence of Q_s can be reconstructed from the x_F-dependence of $p_t^{\rm peak}$. It would be very interesting to compare the function $Q_s(x)$ obtained in p–A collisions in this way with the GBW model one that was obtained from DIS data, in order to establish consistency among the descriptions of all available data. The power λ in $Q_s \sim x^{-\lambda/2}$ determines how strongly the peak varies with x_F. Using $\lambda = 0.3$ as obtained from DIS, which according to a dipole scattering description is compat-

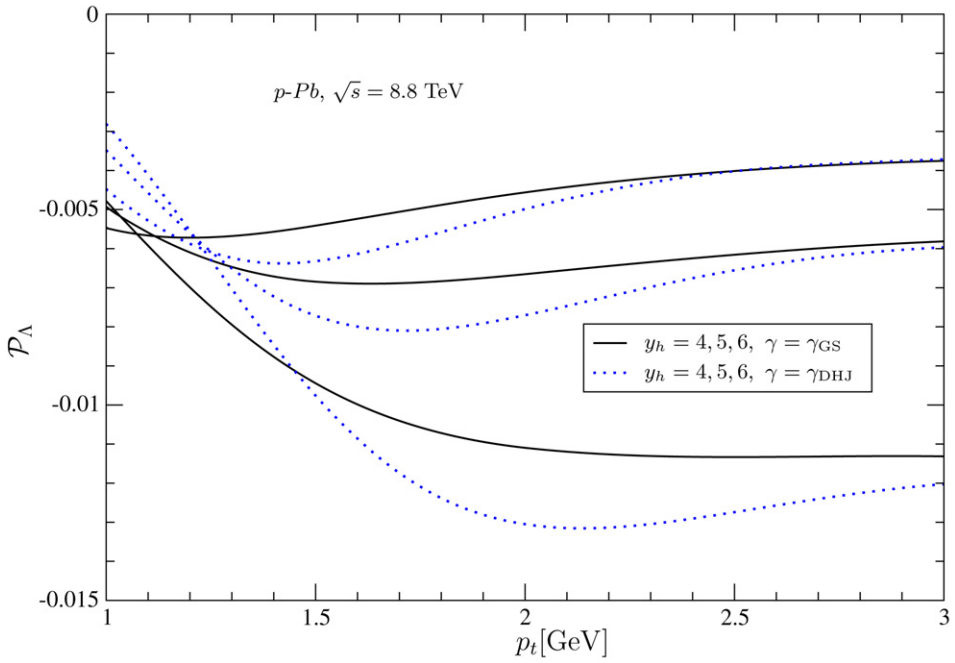

Fig. 6. $\mathcal{P}_\Lambda$ in p–Pb collisions at $\sqrt{s} = 8.8$ TeV, for constant y_h using $\gamma_{\rm GS}$ and $\gamma_{\rm DHJ}$. The top lines correspond to $y_h = 4$, the lowest to $y_h = 6$.

ible with forward hadron production d–Au data of RHIC, we have obtained the following results. In p–Pb collisions at LHC, for values of x_F that are between 0.1 and 0.5, the position of the peak is expected between $p_t = 1.5$ and 2.5 GeV. This result is obtained for a range of dipole models that includes the DHJ and GS models. In p–p collisions, the position of the peak is reduced by a factor of 1.3, but is still in the perturbative regime. In d–Au collisions at RHIC, the position of the peak is smaller by a factor of 2.4 with respect to p–Pb at LHC, due to the much smaller energy. Hence, observing the peak in the perturbative regime at RHIC seems unlikely, except perhaps at even larger x_F values.

For fixed values of the rapidity instead of x_F, the peak in the p_t distribution gets smeared out and is reduced in size. Moreover, in this case the polarization peaks in the perturbative regime $p_t \gtrsim 1$ GeV only for Λ rapidities of 4 or larger in p–Pb collisions at LHC. Therefore, Λ polarization LHC data at fixed x_F are best suited for the purpose of establishing the x-dependence of Q_s in p–A collisions.

Even though the presented quantitative estimates are to some extent model-dependent, the qualitative features of the Λ polarization, i.e. the position of the peak with respect to Q_s and its running with x_F, are expected to be generic for the small-x region. This offers a unique possibility to probe Q_s directly in p–A collisions.

Acknowledgements

We thank Les Bland for fruitful discussions. This research is part of the research program of the “Stichting voor Fundamenteel Onderzoek der Materie (FOM)”, which is financially supported by the “Nederlandse Organisatie voor Wetenschappelijk Onderzoek (NWO)”.

References

[1] M. Anselmino, D. Boer, U. D'Alesio, F. Murgia, Phys. Rev. D 63 (2001) 054029.
[2] P.J. Mulders, R.D. Tangerman, Nucl. Phys. B 461 (1996) 197;
P.J. Mulders, R.D. Tangerman, Nucl. Phys. B 484 (1997) 538, Erratum.
[3] D. Boer, A. Dumitru, Phys. Lett. B 556 (2003) 33.
[4] L. McLerran, R. Venugopalan, Phys. Rev. D 49 (1994) 2233;
L. McLerran, R. Venugopalan, Phys. Rev. D 49 (1994) 3352;
Y.V. Kovchegov, Phys. Rev. D 54 (1996) 5463;
Y.V. Kovchegov, Phys. Rev. D 55 (1997) 5445.
[5] A.H. Mueller, Nucl. Phys. B 558 (1999) 285.
[6] A.H. Mueller, D.N. Triantafyllopoulos, Nucl. Phys. B 640 (2002) 331.
[7] D.N. Triantafyllopoulos, Nucl. Phys. B 648 (2003) 293.
[8] A. Lesnik, et al., Phys. Rev. Lett. 35 (1975) 770.
[9] G. Bunce, et al., Phys. Rev. Lett. 36 (1976) 1113.
[10] A.D. Panagiotou, Int. J. Mod. Phys. A 5 (1990) 1197.
[11] A. Dumitru, J. Jalilian-Marian, Phys. Rev. Lett. 89 (2002) 022301.
[12] L.C. Bland, private communication.
[13] D. de Florian, M. Stratmann, W. Vogelsang, Phys. Rev. D 57 (1998) 5811.
[14] D. Boer, C.J. Bomhof, D.S. Hwang, P.J. Mulders, Phys. Lett. B 659 (2008) 127.
[15] K. Golec-Biernat, M. Wüsthoff, Phys. Rev. D 59 (1999) 014017.
[16] J. Bartels, K.J. Golec-Biernat, H. Kowalski, Phys. Rev. D 66 (2002) 014001.
[17] A. Dumitru, A. Hayashigaki, J. Jalilian-Marian, Nucl. Phys. A 765 (2006) 464.
[18] A. Dumitru, A. Hayashigaki, J. Jalilian-Marian, Nucl. Phys. A 770 (2006) 57.
[19] D. Boer, A. Utermann, E. Wessels, Phys. Rev. D 77 (2008) 054014.
[20] D. Kharzeev, Y.V. Kovchegov, K. Tuchin, Phys. Lett. B 599 (2004) 23.
[21] E. Iancu, K. Itakura, L. McLerran, Nucl. Phys. A 708 (2002) 327.
[22] L.V. Gribov, E.M. Levin, M.G. Ryskin, Phys. Rep. 100 (1983) 1.
[23] E.A. Kuraev, L.N. Lipatov, V.S. Fadin, Sov. Phys. JETP 45 (1977) 199, Zh. Eksp. Teor. Fiz. 72 (1977) 377;
I.I. Balitsky, L.N. Lipatov, Sov. J. Nucl. Phys. 28 (1978) 822, Yad. Fiz. 28 (1978) 1597.
[24] I. Balitsky, Nucl. Phys. B 463 (1996) 99;
Y.V. Kovchegov, Phys. Rev. D 60 (1999) 034008.
[25] H.L. Lai, et al., CTEQ Collaboration, Eur. Phys. J. C 12 (2000) 375.
[26] D. Boer, A. Dumitru, A. Hayashigaki, Phys. Rev. D 74 (2006) 074018.